MEASURING STRUCTURAL PROPERTIES OF GALAXIES IN THE LOCAL UNIVERSE

Paul D. Allen,[1] Simon P. Driver,[1] Jochen Liske,[2] and Alister W. Graham[1]

[1] *Research School of Astronomy and Astrophysics, The Australian National University, Mount Stromlo Observatory, Cotter Rd, Weston, ACT 2611, Australia.*

paul@mso.anu.edu.au

[2] *European Southern Observatory, Karl-Schwarzchild-Str. 2, D-85748, Garching bei München, Germany.*

Abstract The Millennium Galaxy Catalogue provides a representative and complete sample of nearby galaxies for structural analysis. GIM2D is used to model the light profiles for over 10000 resolved galaxies, using three different schemes: $R^{1/4}$+Exponential; $R^{1/n}$+Exponential; $R^{1/n}$. The resulting catalogues are shown to be robust for those galaxies with component half-light radii greater than the seeing.

Keywords: astronomical data bases: catalogues - galaxies: general - galaxies: fundamental parameters - galaxies: structure - galaxies: statistics.

1. Introduction

It has long been known that although galaxies cover an expanse of quite different morphologies, they have tow basic features in common, notably spheroids (or bulges) and disks. These are often observed to have different average colours, metallicities, and kinematics, justifying their treatment as distinct entities. Even at $z \sim 1$, bulges and disks are clearly in place and appear to be the dominant structural feature in the majority of galaxies (Simard et al., 1999; Ravindranath et al., 2004; Barden et al., 2005; Koo et al., 2005; Trujillo et al., 2005). Most models of galaxy formation and evolution involve separate formation scenarios for bulges and disks (e.g. Cole et al., 2000; Kormendy & Kennicutt 2004). It is possible, within the ΛCDM paradigm, to make specific predictions relating the mass and angular momentum of dark matter haloes with the observed distributions in galaxy luminosity and size as a function of redshift (e.g. Mo, Mao, & White 1998, Bouwens & Silk 2004).

Bulge-disk decomposition is therefore a popular and useful method for quantifying the morphologies of galaxies by fitting model surface brightness profiles to data. A bulge-disk model is also convenient because the surface brightness profiles of bulges can be modelled by an $R^{1/4}$ law(de Vaucouleurs, 1948), and exponential profile (Andredakis and Sanders, 1994; de Jong, 1996), or more optimally using a Sérsic profile (Sersic, 1968; Graham & Driver, 2005), and disks are observed to follow exponential laws (de Vaucouleurs, 1959; Freeman, 1970). Finally, software is now available which makes it a fairly straightforward task to perform bulge-disk decomposition on many thousands of galaxies (e.g. Simard et al., 2002; Peng et al., 2002; Trujillo and Aguerri, 2004; de Souza et al., 2004).

Here, we discuss the use of one such publically available bulge-disk decomposition code, GIM2D (Simard et al., 2002), to provide a quantitative measure of the surface brightness profiles of 10095 galaxies in the Millennium Galaxy Catalogue (MGC). This provides a catalogue of structural measurements for a representative and complete sample of galaxies in the ($z \sim 0$) local Universe.

2. The Millennium Galaxy Catalogue

The Millennium Galaxy Catalogue[1] (MGC) is a deep (μ_{lim}=26 B mags/arcsec^2), wide area ($\sim$37.5 deg^2) imaging and redshift survey covering a 0.5 deg wide strip along the equatorial sky from 10h to 14h50$'$. The imaging was carried out using the INT Wide Field Camera (WFC). The survey region overlaps both the 2dFGRS (Colless et al., 2001), and SDSS-DR1 (Abazajian et al., 2003), providing both $u'g'r'i'z'$ photometry, and redshifts for 47.0% of the 10095 resolved galaxies with $B < 20$ mag. The remaining $B < 20$ galaxies without known redshifts were observed as targets in the spectroscopic part of the survey, MGCz. This mostly involved observations using the 2dF instrument on the AAT providing redshifts for a further 47.2% of galaxies in the sample. However, in order to avoid significant redshift incompleteness for objects with low surface brightness (see Driver et al., 2005), both 4-m (ESO/NTT and TNG) and 8-m (Gemini) observations were carried out to obtain spectra for the lowest surface brightness galaxies in the sample.

Comparison between 2dFGRS, SDSS and the MGC shows that the MGC is deeper, more complete, more precise, and of higher spatial resolution than either the 2dFGRS or SDSS-DR1 data sets (Cross et al., 2004; Driver et al., 2005). The increased depth and resolution is demon-

[1]The MGC is publically available at http://www.eso.org/ ~jliske/mgc

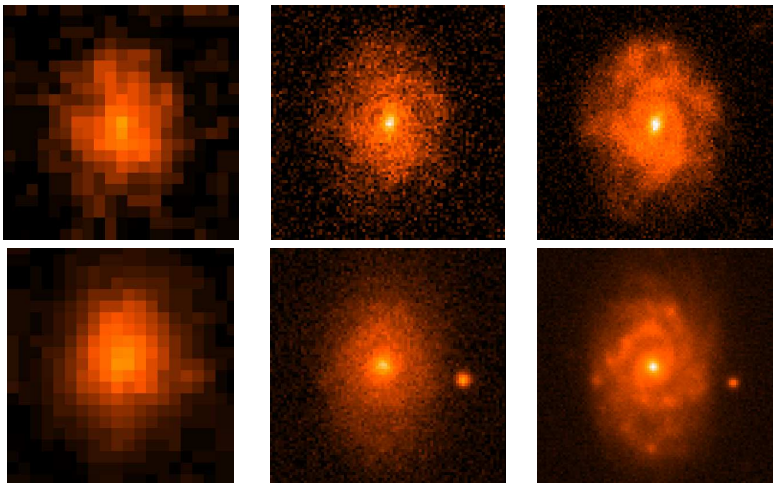

Figure 1. A comparison between Digitized Sky Survey (left, b_J-band), SDSS-DR1 (centre, g-band), and the MGC (right), for MGC18325 (upper panels), and MGC04795 (lower panels).

strated in Figure 1. Full details of the MGC, including observations, data reduction, image detection and classification, are given in Liske et al., (2003). The MGC redshift survey is discussed in detail in Driver et al., (2005).

With a photometric precision of 0.03 mag, astrometric accuracy of 0.08 arcsec (Liske et al., 2003), and 96% redshift completeness to $B_{\rm MGC} = 20$ mag (increasing to 99.8% for $B_{\rm MGC} < 19.2$ mag), the MGC represents an extremely high quality and high completeness census of the nearby galaxy population. It is therefore the ideal data set to use for a detailed analysis of the structural composition of galaxies in the local Universe, and to provide a low redshift anchor for higher redshift studies.

3. Fitting Profiles with GIM2D

In Allen et al., (2005) the 2-D light profiles for all 10095 MGC galaxy images were modelled using the GIM2D package (Simard et al., 2002). GIM2D allows galaxies to be modelled using a single component model, or a two component model with separate profiles for the bulge and disk components. For the MGC, three schemes were used. (1) Sérsic – single component. (2) De Vaucouleurs Bulge + Exponential Disk. (3) Sérsic Bulge + Exponential Disk.

It is important to disentangle the intrinsic morphologies of galaxies from distortions that arise from the combined optical system of telescope, instrument, and atmosphere. Therefore the point spread function (PSF)

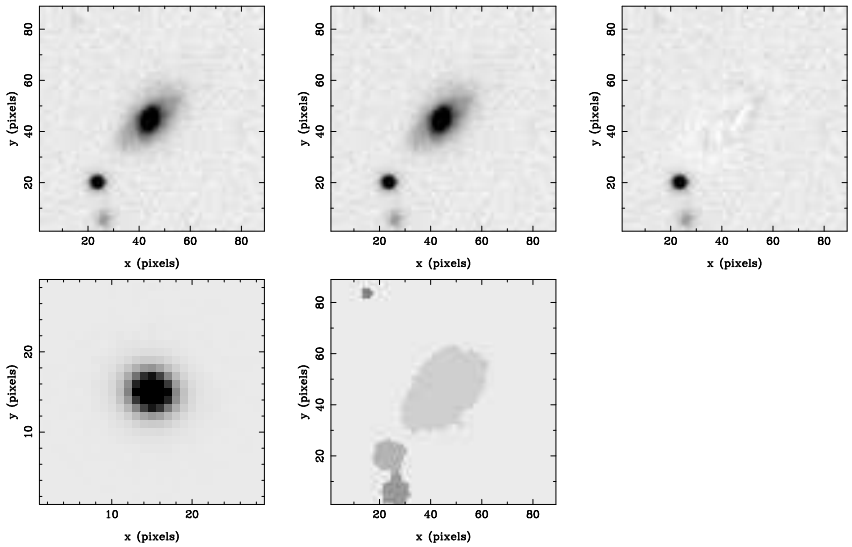

Figure 2. GIM2D input and output for the galaxy MGC27301. The output model shown is for the Sérsic+Exponential fit. The top row shows images of the galaxy (left), the GIM2D model image (centre), and the residual image showing the difference. The bottom row shows the input PSF (left), and the segmentation image or mask (centre).

was also modelled for each galaxy using stars that lie in the same frame as the galaxy. GIM2D then finds the best-fitting PSF-convolved model for each galaxy using the pixels designated as part of the object by the SEXtractor segmentation image mask (see Simard et al., 2002). This resulted in three structural catalogues containing measurements of total flux, bulge to disk flux ratio (B/T), and the $x-y$ position of the central surface brightness. For bulges, effective radii (R_e), Sérsic index (n), ellipticity (ϵ), and position angle (ϕ_b) are all measured. For disks, the catalogues contain measurements of scale-length (h), inclination (i), and disk position angle (ϕ_d). Figure 2 shows example output and residual images for the galaxy MGC27301 along with the raw image, mask, and PSF. Figure 3 shows a plot of the best-fitting model for this galaxy using the Sérsic+Exponential fit.

Quality Control

As an initial test of the accuracy of the GIM2D output, simple global observables such as magnitudes, half-light radii, and $x-y$ centroid positions can be compared to the values measured by other means in Liske et al. (2003). For example, differences between GIM2D output and previous measurements can be indicative of bad segmentation images.

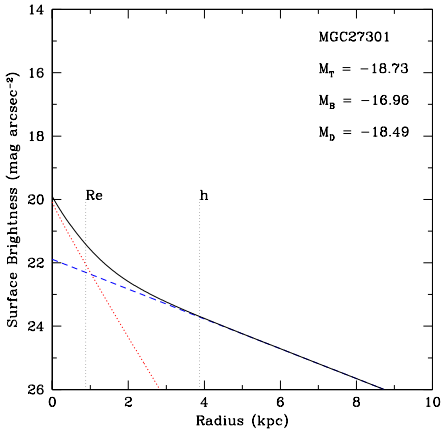

Figure 3. The best fitting profile for MGC27301 (see Figure 2) using the Sérsic+Exponential model. The blue dashed straight line represents the exponential (disk) component, and the red dotted curve corresponds to the Sérsic(bulge) component. The total profile is shown by the solid bold curve. R_e and h are also shown.

If a galaxy has been over-deblended, then the GIM2D magnitude will be an under-estimate. When two nearby galaxies are treated as one, the centroids will be grossly different, and the GIM2D magnitudes over-estimated. It was found that 222 segmentation images needed to be corrected. It is also important to ensure that the fits are interpreted correctly, as the two components can be inverted or used to fit neither a bulge nor a disk (see Allen et al., 2005).

Due to overlaps between pointings of the WFC, 702 objects had duplicate observations. In many cases the observations were carried out on a different night or even as part of different observing runs several months apart. They therefore provide an excellent test of the repeatability of GIM2D fits for a diverse and representative sample of galaxies under different conditions. The comparison reveals that if the half light radius of a component is sufficiently large ($R_e > 0.8\Gamma$ or $1.678h > 0.8\Gamma$ where Γ is the seeing FWHM), then for the Sérsic+Exponential model the standard deviations between repeat measurements are: $R_e \sim 13.2\%$, $\log(n) \sim 13.6\%$, and $h \sim 6\%$. For the component magnitudes: $M_{bulge} \sim 0.24$ mags, and $M_{disk} \sim 0.14$ mags.

4. Summary

The Millennium Galaxy Catalogue is a deep, wide survey of the local galaxy population. Its completeness, depth and resolution make

it ideal for the provision of a representative sample of galaxy structural measurements at $z \sim 0$. GIM2D has been used to obtain the best-fitting Sérsic models, Sérsic+Exponential decompositions, and de Vaucouleurs+Exponential decompositions to the 100095 galaxies with $B < 20$ in the MGC. Structural catalogues are made publically available in Allen et al. (2005). With careful quality control, repeatable measurements are obtainable for galaxies that are larger than the seeing FWHM. The measured parameters can then be used to measure luminosity functions and bivariate brightness distributions (see Liske et al. *this proceedings*).

References

Abazajian, K., et al. (2003). *AJ*, 126:2081–2086.

Allen, P. D., Driver, S. P., Liske, J., Graham, A., Cameron, E., Cross, N. J. G., and de Propris, R. (2005). *MNRAS*, submitted.

Andredakis, Y. C. and Sanders, R. H. (1994). *MNRAS*, 267:283–296.

Barden, M., et al. (2005). astro-ph/0502416.

Bouwens, R. and Silk, J. (2002). *ApJ*, 568:522–538.

Cole, S., Lacey, C. G., Baugh, C. M., and Frenk, C. S. (2000). *MNRAS*, 319:168–204.

Colless, M., et al (2001). *MNRAS*, 328:1039–1063.

Cross, N. J. G., Driver, S. P., Liske, J., Lemon, D. J., Peacock, J. A., Cole, S., Norberg, P., and Sutherland, W. J. (2004). *MNRAS*, 349:576–594.

de Jong, R. S. (1996). *A&AS*, 118:557–573.

de Souza, R. E., Gadotti, D. A., and dos Anjos, S. (2004). *ApJS*, 153:411–427.

de Vaucouleurs, G. (1948). *Annales d'Astrophysique*, 11:247.

de Vaucouleurs, G. (1959). *Handbuch der Physik*, 53:275.

Driver, S. P., Liske, J., Cross, N. J. G., De Propris, R., and Allen, P. D. (2005). *MNRAS*, 360:81–103.

Freeman, K. C. (1970). *ApJ*, 160:811.

Graham, A. W. and Driver, S. P. (2005). *PASA*, 22:118.

Koo, D. C., et al (2005). *ApJS*, 157:175–217.

Kormendy, J. and Kennicutt, R. C. (2004). *ARAA*, 42:603–683.

Liske, J., Lemon, D. J., Driver, S. P., Cross, N. J. G., and Couch, W. J. (2003). *MNRAS*, 344:307–324.

Mo, H. J., Mao, S., and White, S. D. M. (1998). *MNRAS*, 295:319–336.

Peng, C. Y., Ho, L. C., Impey, C. D., and Rix, H. (2002). *AJ*, 124:266–293.

Ravindranath, S., et al (2004). *ApJL*, 604:L9–L12.

Sersic, J. L. (1968). *Atlas de galaxias australes*. Cordoba, Argentina: Observatorio Astronomico, 1968.

Simard, L., et al (1999). *ApJ*, 519:563–579.

Simard, L., et al (2002). *ApJS*, 142:1–33.

Trujillo, I. and Aguerri, J. A. L. (2004). *MNRAS*, 355:82–96.

Trujillo, I., et al (2005). astro-ph/0504225.